

論文 / 著書情報  
Article / Book Information

Title	EFFECTS OF MASONRY INFILL WALLS ON THE SEISMIC BEHAVIOR OF A TYPICAL RC BUILDING IN NEPAL.
Authors	Sujan PRADHAN, Yuebing LI, Yasushi SANADA, Haruka KATAYAMA, Shinya FUKUI, Krishna Kumar BHETWAL, Ho CHOI, Yo HIBINO, Koichi KUSUNOKI
Pub. date	2020, 9
Citation	2020 17WCEE Proceedings



## EFFECTS OF MASONRY INFILL WALLS ON THE SEISMIC BEHAVIOR OF A TYPICAL RC BUILDING IN NEPAL

S. Pradhan<sup>(1)</sup>, Y. Li<sup>(2)</sup>, Y. Sanada<sup>(3)</sup>, H. Katayama<sup>(4)</sup>, S. Fukui<sup>(5)</sup>, K.K. Bhetwal<sup>(6)</sup>, H. Choi<sup>(7)</sup>, Y. Hibino<sup>(8)</sup>, K. Kusunoki<sup>(9)</sup>

<sup>(1)</sup> PhD Candidate, Graduate School of Engineering, Osaka University, Osaka, Japan, [sujan\\_pradhan@arch.eng.osaka-u.ac.jp](mailto:sujan_pradhan@arch.eng.osaka-u.ac.jp)

<sup>(2)</sup> Lecturer, School of Civil Engineering and Architecture, Northeast Electric Power University, Jilin, China, [sdlybing@hotmail.com](mailto:sdlybing@hotmail.com)

<sup>(3)</sup> Professor, Graduate School of Engineering, Osaka University, Osaka, Japan, [sanada@arch.eng.osaka-u.ac.jp](mailto:sanada@arch.eng.osaka-u.ac.jp)

<sup>(4)</sup> Former Graduate Student, Graduate School of Engineering, Osaka University, Osaka, Japan, [katayama.haruka@takenaka.co.jp](mailto:katayama.haruka@takenaka.co.jp)

<sup>(5)</sup> Former Graduate Student, Graduate School of Engineering, Osaka University, Osaka, Japan, [fukui\\_shinya@arch.eng.osaka-u.ac.jp](mailto:fukui_shinya@arch.eng.osaka-u.ac.jp)

<sup>(6)</sup> Researcher, Structural and Earthquake Engineering Research Institute, Kathmandu, Nepal, [krishbhetwal@gmail.com](mailto:krishbhetwal@gmail.com)

<sup>(7)</sup> Associate Professor, Faculty of Science and Technology, Shizuoka Institute of Science and Technology, Shizuoka, Japan, [choi.ho@sist.ac.jp](mailto:choi.ho@sist.ac.jp)

<sup>(8)</sup> Associate Professor, Graduate School of Engineering, Hiroshima University, Hiroshima, Japan, [hibino@hiroshima-u.ac.jp](mailto:hibino@hiroshima-u.ac.jp)

<sup>(9)</sup> Professor, Earthquake Research Institute, The University of Tokyo, Tokyo, Japan, [kusunoki@eri.u-tokyo.ac.jp](mailto:kusunoki@eri.u-tokyo.ac.jp)

### Abstract

A large number of Nepalese reinforced concrete (RC) buildings were significantly damaged by the Nepal earthquake of magnitude (Mw) 7.8 on April 25, 2015. Several specific characteristics of Nepalese RC buildings might be responsible for such damage. The specific characteristics of RC residential buildings with brick masonry infill walls in the capital city of Nepal, Kathmandu, are the focus of the current study. Evaluation of the effect on and the interaction of the masonry infill wall with the surrounding RC frame is a complex task for the designer. Hence, Nepalese RC buildings with infill walls are designed as bare frames by neglecting the stiffness and strength contributions of the infill walls. However, previous studies have shown that infill walls also affect the seismic performance of this type of structure. Hence, the main objective of the current study is to investigate and clarify through observation, experimentation and analysis the alteration of the seismic performance of Nepalese RC buildings due to the presence of masonry infill walls. First, the vibration characteristics of a typical RC residential building in Kathmandu as well as the engineering properties of the nearby ground surface were investigated based on microtremor measurements. Second, the mechanical properties of brick masonry prism specimens representing masonry walls in the buildings were experimentally investigated. In addition, an analytical study with three different contributions of infill walls to the RC frame was conducted to investigate their effects on the vibration characteristics and the seismic performance of the building. For analysis case A, the building was analyzed as a bare frame neglecting the infill walls, while only the weight of the infill walls and the weight, strength and stiffness of the infill walls were considered for cases B and C, respectively. As a result, the vibration characteristics obtained from analytical case C agreed well with the microtremor measurement results, clarifying the effects of the infill walls on the building behavior. Moreover, it was confirmed that the presence of the masonry infill walls decreased the natural vibration period; however, the infill walls increased the lateral resistance parallel to the in-plane direction, reducing the building seismic response in displacement. These findings will contribute to estimating the seismic performance of Nepalese RC buildings more accurately and hence minimize future earthquake disasters.

*Keywords: Microtremor measurement; Nonstructural wall; Numerical analysis; Prism test; Strut replacement*



## 1. Introduction

Nepal is a country with a high risk of earthquakes located at the boundary between the Indian and Eurasian (Tibetan) tectonic plates. On April 25, 2015, at 11:56 (Nepal standard time), a strong earthquake of magnitude ( $M_w$ ) 7.8 hit Nepal with an epicenter east of Gorkha district, Barpak village, known as the Gorkha earthquake [1]. The hypocenter was at an approximate depth of 8.2 km and was the worst earthquake since the 1934 Nepal-Bihar earthquake. The main shock also jolted some parts of China, India and Bangladesh. A strong aftershock of magnitude ( $M_w$ ) 7.3 also affected Nepal on May 12, which led to further damage to the structures. Many reinforced concrete (RC) buildings, especially in the capital city of Nepal, Kathmandu, were damaged [2]. The presence of brick masonry infill walls is the specific characteristic of Nepalese RC buildings that might be responsible for such damage. Since brick walls are economical and easy to construct, RC buildings with brick masonry infill walls are abundant in other countries with high seismicity, such as China and Turkey.

The estimation and evaluation of the failure modes of the masonry infill wall as well as its interaction with the surrounding frames is a complex task. Additionally, there is still a lack of knowledge among designers about the role of the infill wall in the seismic performance of RC buildings. Hence, when designing buildings, the contribution of infill walls to Nepalese RC buildings is only the self-weight as a nonstructural element, neglecting its strength and stiffness. However, previous studies [3,4] have revealed that infill walls also affect the seismic performance of the whole structure. Hence, designing an RC building by neglecting the effects of infill walls may lead to an inaccurate estimation of the overall performance of the building. This fact leads to unexpected severe damage to building during an earthquake in modes different from those predicted. Since masonry infill walls are widely used in existing and new buildings, it is very important to recognize their effect on the seismic performance of RC buildings to mitigate severe damage to buildings during earthquakes. Hence, to clarify the effects of infill walls on Nepalese RC buildings, the vibration characteristics of a typical RC residential building with brick masonry infill walls in Kathmandu as well as the engineering properties of the nearby ground were investigated based on microtremor measurements. In addition, experimental studies were carried out to investigate the mechanical properties of brick masonry specimens representing infill walls in the building. Moreover, analytical studies of three different contributions of infill walls to the RC frame were performed to investigate their effects on the vibration characteristics and the seismic performance of the RC building. A comparison between the analytical results and the microtremor measurement results revealed that the vibration characteristics of the RC building were significantly affected by the presence of masonry infill walls; hence, while designing buildings, it is necessary to consider the effect of masonry infill walls.

## 2. Target Building

After the 2015 Gorkha earthquake, a team of authors was dispatched to perform a field investigation to investigate the damage to and examine the seismic capacity of Nepalese buildings (especially RC buildings in Kathmandu). The team consisted of professors and experts who specialized in RC buildings and earthquakes. For the detailed investigations, an RC residential building (ref. as the target building) with brick masonry infill walls was selected. The target building was located in Shitapaila, in the western part of Kathmandu, as shown in Fig. 1, and was constructed after the Gorkha earthquake. The building was a common RC residential building that had five stories of superstructure, including the ground floor and one underground story with a mat foundation. Originally, this building was designed as a 3-story building, but it was extended to 5 stories during construction. Fig. 2 shows the southeast and northeast views of the building. Fig. 3 shows the ground floor plan and the sectional elevation along the X-X' axis. The building had 4 bays and one bay in the longitudinal and transverse directions, respectively, as shown in Fig. 3. The exterior brick masonry infill walls were utilized in the longitudinal direction of the building (mainly windows and doors in the transverse direction). Plaster finishings on both sides of the infill walls were used on the northwest side;



however, plaster finishing on one side of the wall (no plaster on outside of the wall, as shown in Fig. 2a) was used on the southeast side of the building.

The concrete strength of the building was evaluated as 39.8 MPa via an onsite nondestructive test. Since the information regarding the reinforcement type was not available, reinforcement ( $f_y = 415$  MPa), which is widely used for RC buildings in Nepal, was used for the analysis. The slab thickness was 160 mm. Fig. 4 shows the cross-sectional details of the beams and columns of the building.

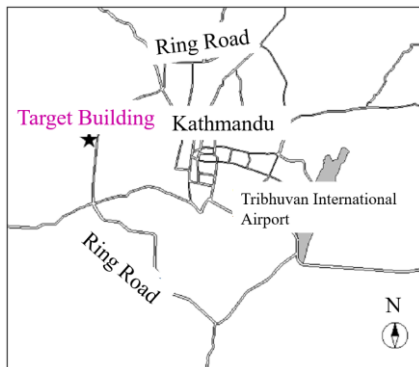
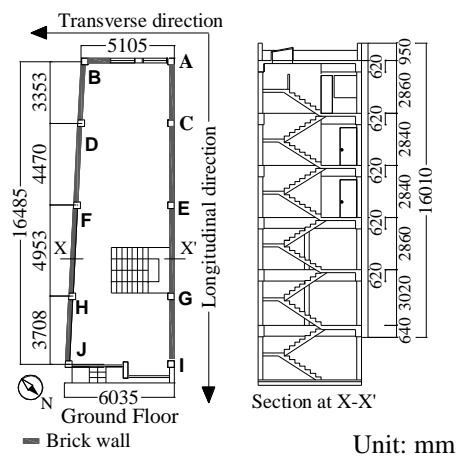


Fig. 1 - Location map of the target building

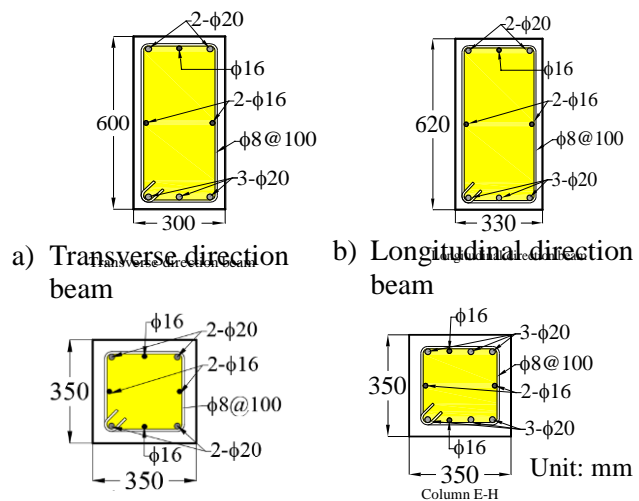


a) Southeast view      b) Northeast view  
Fig. 2 - Overview of the target building



a) Ground floor plan      b) Sectional elevation along X-X'

Fig. 3 - Ground floor plan and sectional elevation of the target building



a) Transverse direction beam      b) Longitudinal direction beam  
c) Column A-D, I, J      d) Column E-H  
Fig. 4 - Beam and column cross-sections

### 3. Microtremor Observation

#### 3.1 Measurement method

Microtremor measurement is a simple method to investigate the vibration characteristics of existing buildings and the ground by a nondestructive method. The main advantages of the microtremor measurement method are its simple analyses, efficiency, accuracy, ability to temporally and stably estimate frequency and quick operation [5]. To predict the seismic response of the target building (the vibration characteristics, i.e., the natural period and the mode shape of the building), the microtremor measurement was performed in



October 2015 using a portable microtremor instrument. For the measurement, the instrument made by Kinkei system corporation, Osaka, Japan (speed type seismic sensor; simultaneous measurement of 3 components: 2 horizontal and 1 vertical; natural vibration frequency: 2 Hz; measurement amplitude:  $\pm 2$  mm; sensitivity: 0.8 V/kine; 100 speed data records per second) and the recorder were used.

To investigate the ground dynamic characteristics, microtremor measurements were performed at two relatively flat locations approximately 30 meters southwest of the building. For the building, as shown in Fig. 5, the microtremor sensors were set at a fixed distance from the central column at the western side columns of the building. Fig. 5 also shows the microtremor sensor at the state of measurement. To examine the change in vibration characteristics depending on the floors and to obtain the mode shape of the building, three measuring instruments were used. Two instruments were fixed on the ground floor (G.F) and the top floor (4<sup>th</sup> floor), whereas the remaining instrument was planned to move from the first floor to the rooftop (R.T). Hence, four cases of measurement were investigated, as shown in Fig. 6. Due to the limitation of the measuring instrument (GPS signal is essential), the underground floor was not measured. For each case, multipoint simultaneous measurements were performed with the help of the GPS attached to the recorder. To obtain stable data, the measurement was recorded for 15 minutes for each case. The measurement was performed in the morning when the vibration due to the traffic was relatively low and no interior construction works were being performed.

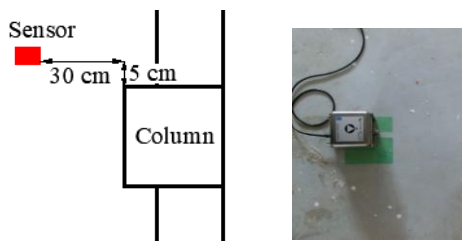


Fig. 5 - Position and setup of microtremor sensors in the building

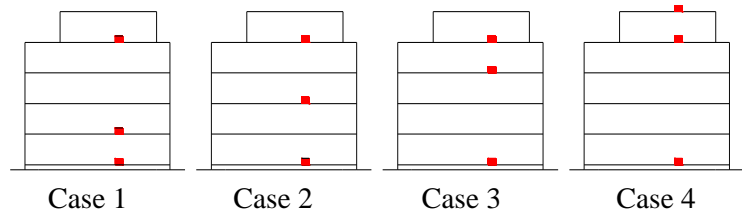


Fig. 6 - Cases for microtremor measurement

### 3.2 Vibration characteristics based on measurement

Relatively steady vibration data (approximately 165 seconds) were taken among the measured data (approximately 900 seconds), and spectral analyses were performed. Fig. 7 shows the typical speed data used for the spectral analyses for case 1 in Fig. 6.

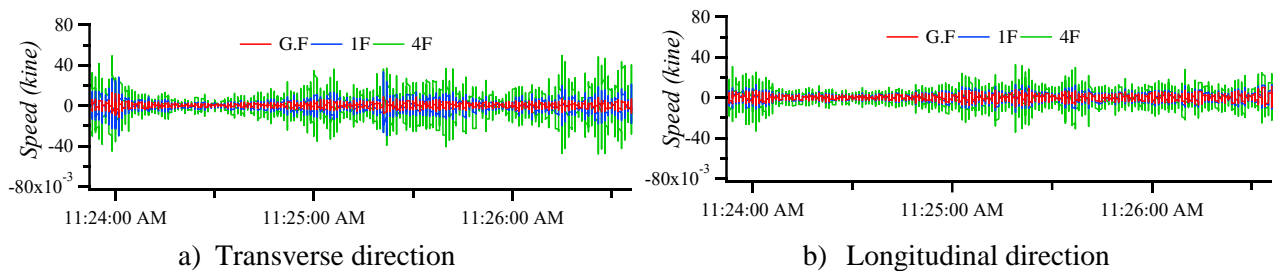


Fig. 7 - Time history wave form of the original measurement (case 1)

#### 3.2.1 Natural period of the ground

The horizontal/vertical (H/V) spectrum ratio is a simple and quick way to obtain the engineering properties of a site by measuring the field ambient noise wave with a single three-component sensor. This method is used for the rapid estimation of the fundamental resonance frequency of the site. In this research, by using the microtremor measurements of the immediate ground in the vicinity of the target building, the Fourier spectra of the recorded seismic noise for all three components (east-west, north-south and vertical) were evaluated. The H/V spectrum ratio was evaluated by dividing the square root of the sum of the square of the



two horizontal Fourier amplitudes by the vertical Fourier amplitude. This division of the horizontal and vertical components resulted in the H/V curve being a function of frequency, as shown in Fig. 8. The natural frequency (natural period) of the ground measured in two nearby locations was evaluated as 1.14 Hz (0.88 seconds) and 1.03 Hz (0.97 seconds). These data show that the natural periods were greater than 0.6 seconds; hence, the underlying ground of the target building was categorized as type III (soft soil sites) according to the NBC [6].

### 3.2.2 Natural period of the building

Fig. 9 shows the result of the Fourier spectrum of the horizontal component of each floor for measurement case 1. Fig. 10 shows the ratios of the horizontal Fourier spectrum component of the upper floor to that of the G.F in the transverse and longitudinal directions for each case. From Fig. 10, the natural frequency of the building in the transverse direction was evaluated as 2.92 to 2.98 Hz, and the natural period was 0.33 to 0.34 seconds. However, a distinct vibration frequency could not be obtained in the longitudinal direction; it was estimated to be 7.29 to 9.36 Hz (0.11 to 0.14 seconds). This finding shows that the natural period in the longitudinal direction was much shorter than that in the transverse direction. The existence of the brick masonry infill walls in the longitudinal direction but the presence of almost no infill walls in the transverse direction (as shown in Fig. 3) was considered the main reason for shorter natural period in the longitudinal direction. As shown in Fig. 10, the peak secondary natural frequency clearly appeared in the transverse direction (6.24 Hz), whereas it did not appear in the longitudinal direction.

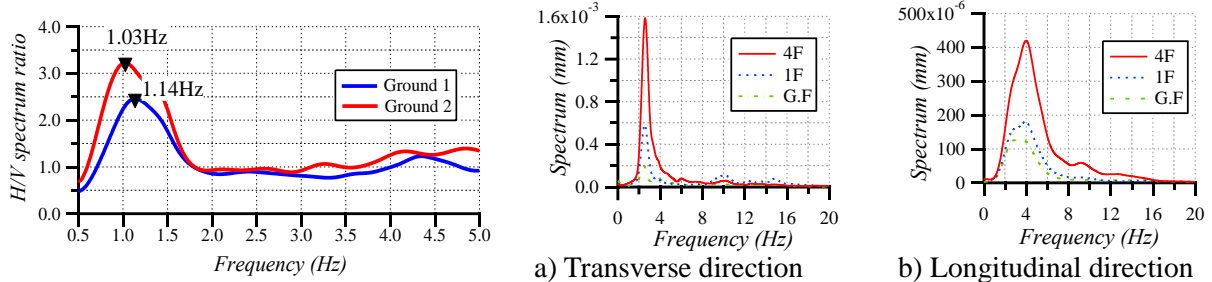


Fig. 8 - H/V Spectrum ratio of the ground

Fig. 9 - Fourier spectrum of measurement (case 1)

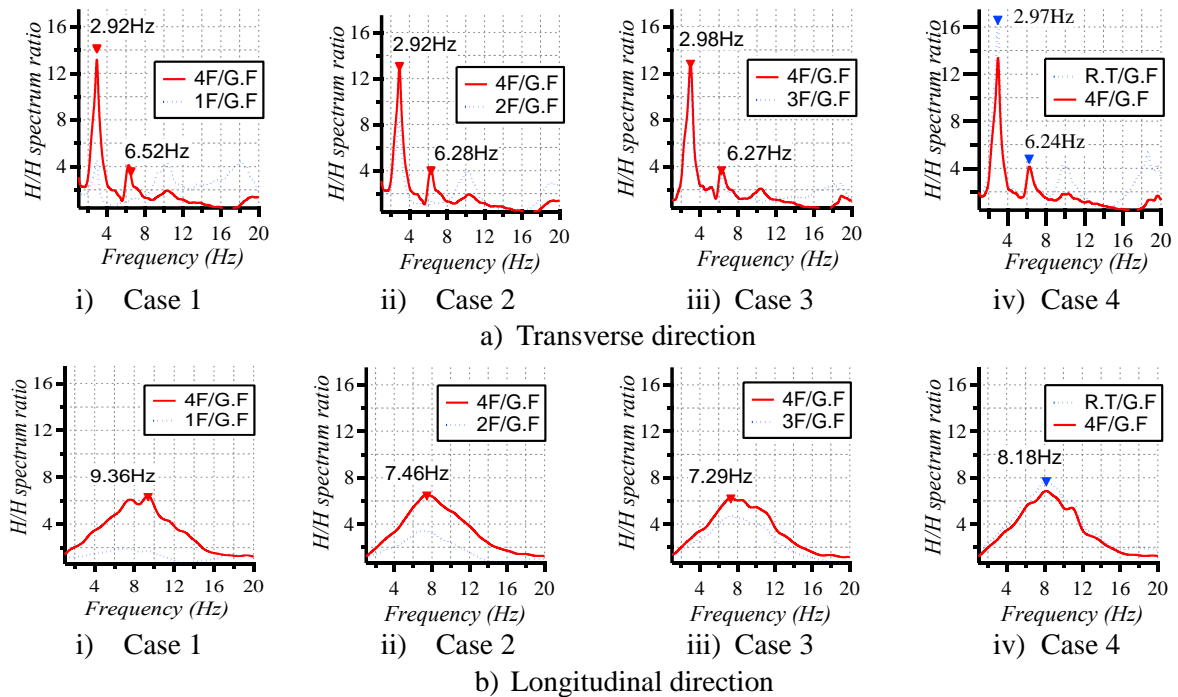


Fig. 10 - H/H spectrum ratio of the upper floor to the ground floor for each measurement case



### 3.2.3 Mode shape of the building

Based on the results of each measurement case as explained above, the mode shape of the building in the vertical direction was evaluated. For the evaluation, the maximum Fourier spectrum obtained in each measurement case was set as the reference measurement level. The phase difference between the reference floor and the other measurement floors was evaluated by the difference in  $\Delta\theta$  of the Fourier spectrum, whereas the amplitude was evaluated by multiplying the amplitude spectrum by  $\cos\Delta\theta$ . To obtain the mode shape, the amplitude of each floor was subtracted from that of the ground floor by assuming the foundation to be fixed. By this standardization of the maximum evaluated amplitude of each floor and by plotting them in the vertical direction, the mode shape was obtained as shown in Fig. 11 i) -iv). In the figure, the solid line represents the primary mode shape, whereas the broken line represents the secondary mode shape. Fig. 12 shows the primary mode shape of the building in the longitudinal direction. In Fig. 11 and Fig. 12, the results from the analysis, which will be discussed later in Section 5.2, are also shown. The mode shape of each measurement case (each floor) as well as from the analysis was standardized based on the method suggested by Shibata A [7], and the equivalent mode shape of the building was evaluated as shown in Fig. 11 v) and Fig. 12 v).

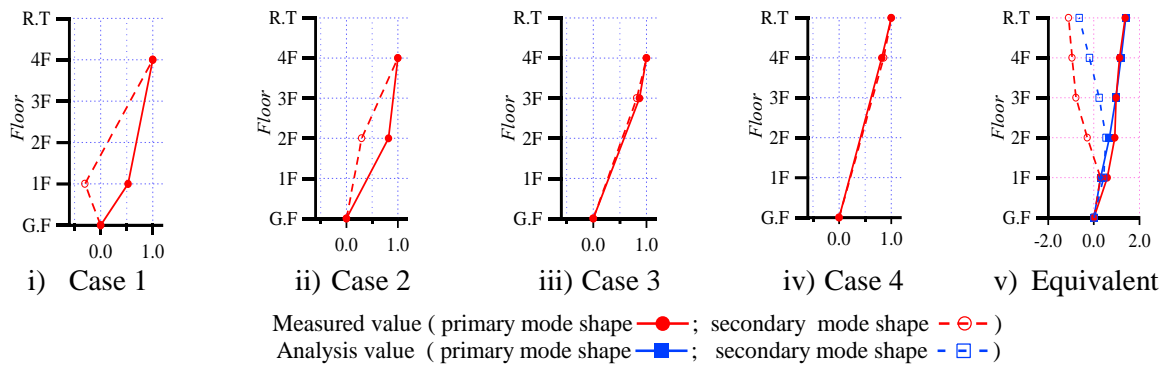


Fig. 11 - Mode shapes in the transverse direction

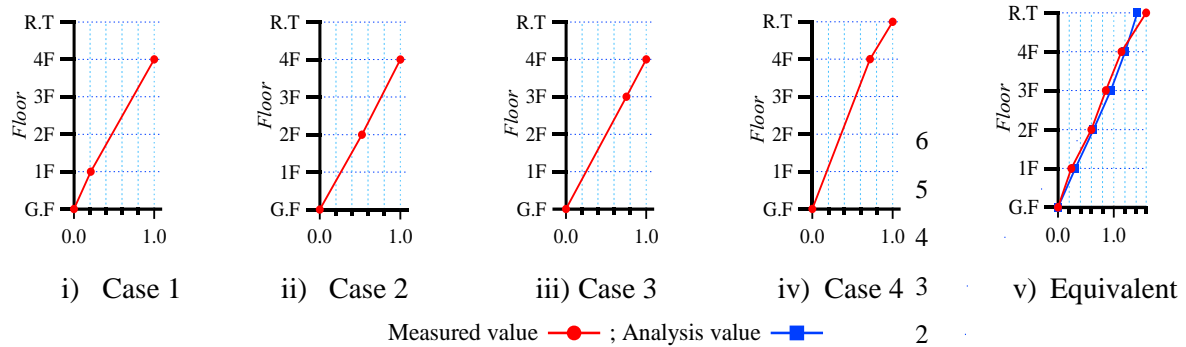


Fig. 12 - Mode shapes in the longitudinal direction. 1

## 4. Experimental Investigation on the Mechanical Properties of Brick Masonry Walls

The mechanical properties of the masonry wall highly depend on the properties of the material used as well as on the workmanship of the mason. Hence, in this research, the brick masonry prism specimens were prepared in the same manner as the brick masonry infill walls used in the target building for the experimental studies. The brick masonry prism specimens were used to represent the brick masonry infill walls in the target building. The specimens were prepared by the same local masons engaged in the construction of the building with the same materials and process applied as those of the target building. Experimental studies were conducted to obtain the density, strength and elastic moduli of the brick masonry walls for the subsequent numerical studies.



#### 4.1 Specimen and test setup

Brick masonry infill walls with two types of finishing conditions, i.e., one side plastered and both sides plastered, were used in the target building at the state when the microtremor measurement described in Section 3 was performed. The plaster finishing works were made of cement and sand mortar, which might affect the strength and deformation characteristics of the brick masonry wall. Hence, to investigate the effects of the plaster finishing works on the mechanical characteristics of the brick masonry walls, three kinds of specimens with three different types of plaster finishing (N without plaster, O with one side plastered, B with both sides plastered) were prepared for compression tests, as shown in Fig. 13. The bricks used were burnt bricks with a size of 220 mm × 110 mm × 55 mm. The mix proportion for the joint mortar was a cement: sand ratio of 1:4, and that for the plaster mortar was 1:5, with a water-to-cement ratio of 0.85 (approx.). However, the water-to-cement ratio was not measured accurately, as it was arranged as per the experience of the masons. The thickness of the plaster was approximately 13 mm. The weight density of the brick masonry walls for different plaster finishing conditions, i.e., without plaster, one side plastered and both sides plastered, were determined to be 17.5, 17.7 and 18.0 kN/m<sup>3</sup>, respectively, from its measured weight and volume.

The experiments were conducted at the Material Laboratory in Tribhuvan University, Pulchowk Campus, Nepal, using a universal testing machine (UTM). The measurements were applied loads and strains in the horizontal and vertical directions. The strains in the horizontal and vertical directions were measured by displacement transducers attached to the specimen, as shown in Fig. 14. Fig. 15 shows a photograph of the compression test during the experiment.

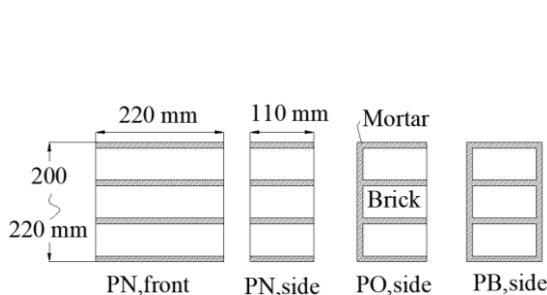


Fig. 13 - Specimen dimensions

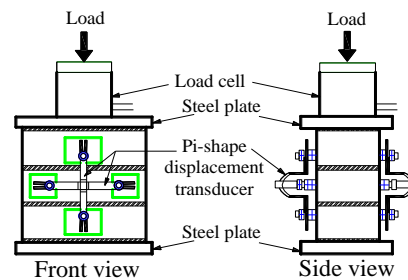


Fig. 14 - Test setup.



Fig. 15 - Experiment.

#### 4.2 Experimental results

The values of the elastic moduli and compressive strengths from the compression tests are summarized in Table 1. The compressive strength of the brick masonry wall was evaluated by dividing the maximum load by the gross cross-sectional area (including plaster) of the specimen. The compressive strain was obtained by dividing the output of the vertical displacement transducer by its gauge length. The compressive stress-strain relationships of all the brick masonry prism specimens are shown in Fig. 16. As shown in Fig. 16 a), the elastic modulus of PN3 was much lower than that of the other two specimens; hence, the test results of PN3 were not included to evaluate the average compressive strength and the elastic modulus of the PN series because it was considered unreliable. The elastic modulus presented in Table 1 was the initial slope with the approximate linear stiffness of the stress-strain relationships shown in Fig. 16. From the table, it is clear that the elastic moduli of the PB series with plaster finishing on both sides was significantly higher than those of the PN and PO series without plaster and with plaster on one side, respectively. However, the explicit effect of plaster finishing works on the compressive strength of brick masonry walls was not observed in this series of tests. Hence, these tests showed that the elastic modulus of the brick masonry wall was significantly affected, whereas the plaster finishing work did not have any obvious effect on the compressive strength of the wall.



Table 1 - Results of compression tests

	Elastic Modulus (N/mm <sup>2</sup> )	Compressive strength (N/mm <sup>2</sup> )	Consideration for average evaluation
PN1	2192	5.1	Considered
PN2	2278	3.0	Considered
PN3	795	3.7	Not considered
<b>Average</b>	<b>2235</b>	<b>4.1</b>	
PO1	2108	2.7	Considered
PO2	2032	3.2	Considered
PO3	1935	1.6	Considered
<b>Average</b>	<b>2025</b>	<b>2.5</b>	
PB1	4777	3.4	Considered
PB2	5394	2.0	Considered
PB3	6506	4.3	Considered
<b>Average</b>	<b>5559</b>	<b>3.2</b>	

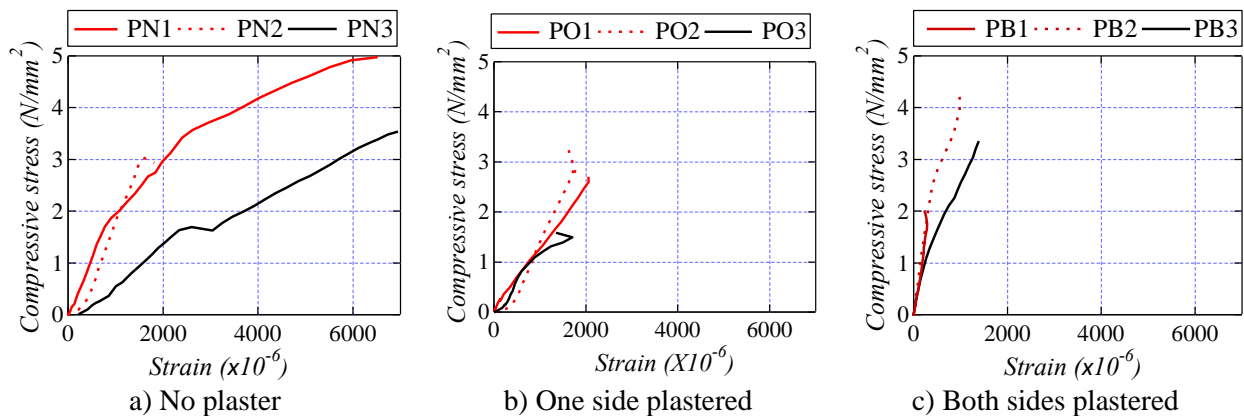


Fig. 16 - Stress-strain relationships from compression tests

## 5. Analytical Seismic Performance Evaluation of the Building

Numerical analyses were performed by replacing each column and beam with a line element representing the inelastic flexural and elastic axial/shear behavior. To investigate the effect of infill walls on the seismic performance of the building, an analytical study with three different contributions of infill walls to the RC frame was performed. The consideration of the weight, strength and stiffness of the infill wall for each analytical case is summarized in Table 2. The structural characteristics of infill brick masonry walls referred to the experimental results of brick masonry prism specimens as described in Section 4.2. The self-weight of the brick masonry infill wall was evaluated by multiplying its volume by the respective weight density in Section 4.1.

Table 2 - Consideration of infill walls for analytical cases

Analysis case	Weight of brick walls	Stiffness and strength of brick walls
Case A	Neglected	Neglected
Case B	Considered	Neglected
Case C	Considered	Considered



### 5.1 Building modeling for analytical studies

The building was modeled based on the following assumptions:

- 1) The 5-story superstructure, neglecting the basement, was represented by the line elements. The footing beams were assumed to be rigid, and the foundations were replaced by pin supports under the footing beam elements. The rigid zones of the line elements were set up from the node to  $D/4$  from the member critical section ( $D$ : depth of each member). The restoring force characteristics were evaluated based on the spring models [8], as summarized in Table 3.

Table 3 - Modeling for restoring the force characteristics of the column and beam

Members	Bending	Shear and Axis
Column	Multi-spring model	Uniaxial elastic spring
Beam	Uniaxial inelastic spring	Uniaxial elastic spring

- 2) The weight, stiffness and strength of the infill walls were considered for analytical case C. The infill wall was replaced by a line (strut) element with pins at both ends. The wall stiffness was evaluated by using the width of the strut ( $w_s$ ) given by Smith & Carter [9], as shown in Eq. (1). The strut strength was evaluated by using the width ( $w_m$ ) given by Mainstone [10] in Eq. (2). The evaluated strut strength by using the width ( $w_s$ ) provided by Smith & Carter was larger than that evaluated by using the width ( $w_m$ ) provided by Mainstone. Hence, the compressive strength of the wall from the compression test was reduced so that the strength of the strut having the width obtained by Eq. (1) was the same as that having the width obtained by using Eq. (2).

$$w_s = 0.58 \left( \frac{1}{H} \right)^{-0.445} (\lambda_h H')^{0.335} d_z \left( \frac{1}{H} \right)^{0.064} \quad (1)$$

$$w_m = 0.175 d_z (\lambda_h H')^{-0.4} \quad (2)$$

where  $\lambda_h$  is a nondimensional parameter expressing the relative stiffness of the surrounding frame to the infill wall and can be evaluated by using Eq. (3).

$$\lambda_h = \left[ \frac{E_z t \sin 2\theta}{4E_b I_s H} \right]^{\frac{1}{4}} \quad (3)$$

The meanings of the symbols are as shown in Fig. 17.

- 3) For modeling the infill wall, it was replaced by the equivalent strut elements with the elastic modulus and compressive strengths as explained in point 2. Infill walls with openings were represented by an equivalent strut with a reduced wall thickness.
- 4) A bilinear model linking the origin to the yield point with a straight line was used to restore the force characteristics of the strut representing the infill wall. The postyield stiffness of the strut was assumed to be 0.1% of the elastic modulus [11] by assuming the force-deformation characteristics of the strut were similar to those of the structural wall. The analytical models based on the above assumptions are shown in Fig. 18.

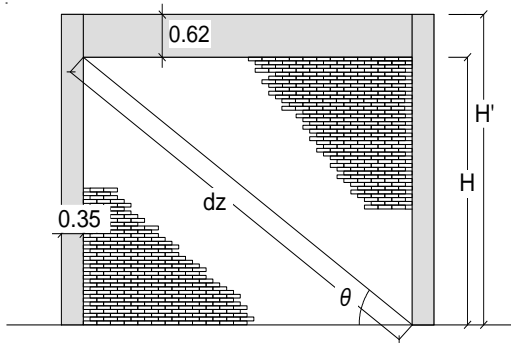


Fig. 17 - Symbol reference diagram for the infill wall

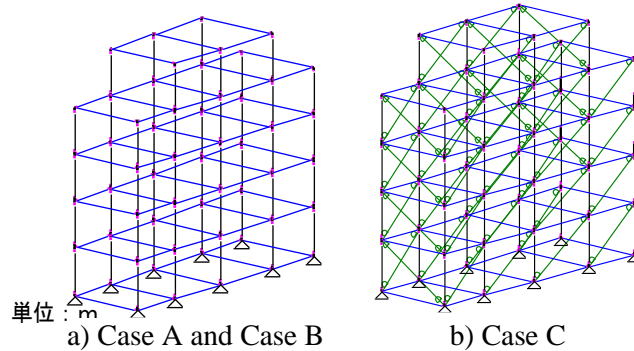


Fig. 18 - Analytical modeling

## 5.2 Comparison of the vibration characteristics from analysis and microtremor measurement

Eigenvalue analyses were performed for all the analytical cases in both transverse and longitudinal directions, and the results were compared with the microtremor measurement results, as shown in Table 4. The mode shapes of the building from the analysis (Case C) and the microtremor measurement were compared, as shown in Fig. 11 and Fig. 12. These findings show that the mode shapes from the analysis and the measurement had good agreement, especially for the primary mode shape. Table 4 shows that the natural periods of Case C considering the weight, stiffness and strength of the infill wall had the smallest and closest values to those of the microtremor measurements, which clarifies that the vibration characteristics of Nepalese RC buildings were significantly affected by the masonry infill walls.

Pushover analyses were performed in the longitudinal direction, and the load was applied from the northeast to southwest direction up to the maximum story drift of 5% rad. Case C, with the struts representing masonry infill walls, had the highest yield strength among all three cases: 1.5 times higher than that of Case A and 2.5 times higher than that of Case B, as shown in Fig. 19. This result indicated that the strength of the building was significantly increased when the infill walls were considered, as in Case C. Hence, these findings clarified that the effect of the infill wall should be considered when designing a RC building, as the seismic performance of the RC building was greatly affected by different considerations of the infill wall, as shown in Table 4 and Fig. 19.

Table 4 - Comparison of the elastic natural periods

Natural period (s)	Measured value	Analysis value		
		Case A	Case B	Case C
Transverse direction	0.33~0.34	0.498	0.646	0.268
Longitudinal direction	0.11~0.13	0.420	0.546	0.138

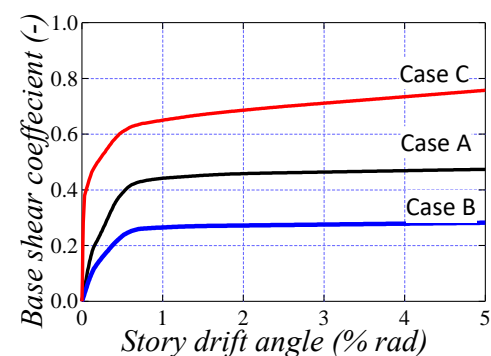


Fig. 19 - Comparison of strength

## 5.3 Replacement with the equivalent single-degree-of-freedom system

To compare the design response spectrum and the evaluated response, the results of the pushover analyses were replaced with the static performance curves ( $S_a$ - $S_d$  relationships) in the form of the equivalent single-degree-of-freedom systems based on past research [12]. Furthermore, the obtained performance curve was



idealized by an elasto-plastic bilinear curve with an equivalent energy dissipation capacity to that of the performance curve.

#### 5.4 Design response spectrum used in Nepal and the comparison of earthquake resistance

Structural design in Nepal was performed by referring to Indian Standards (IS) before the introduction of the Nepal National Building Code (NBC) in 1994. The IS code is the origin [13] of NBC. Since the target building was constructed in 2015, the structural design was performed according to the NBC and IS codes. Thus, in this study, an acceleration response spectrum for the target building was evaluated according to IS [14]. The acceleration response spectrum in IS [14] for different types of soil is shown in Fig. 20 in the form of the acceleration-displacement ( $S_a$ - $S_d$ ) response spectrum. As explained in Section 3.2.1, the soil beneath the target building was categorized as Type III (soft soil).

Fig. 21 shows the response points estimated for the three analytical cases evaluated by overlaying the bilinear curve obtained in Section 5.3 on the design spectrum curve of IS [14]. To represent the inelastic response, the response spectra assumed at 5% damping (red lines in Fig. 21) were reduced for higher damped response spectra (blue lines in Fig. 21). The reduced response spectrum was evaluated by using the method suggested by Shibata A [15]. The response point is defined by the intersection point of the capacity curve and the reduced response curve at which the capacity and demand are the same, as shown in Fig. 21.

Case A, having only the RC frame, responded at 0.33 meter in displacement and 6.78 in ductility factor. Case B, considering the weight of the infilled walls, responded at 0.53 meter in displacement and 7.18 in ductility factor, exhibiting higher displacement than that of Case A. Case C, in which the weight, strength and stiffness of the infilled walls were considered, showed the lowest value of displacement of 0.24 meter, which was approximately 0.75 and 0.5 of those in case A and case B, respectively and 5.09 in ductility factor. These results showed that the displacement response of the building was reduced due to the presence of the brick masonry infill walls, as in Case C. Thus, the response displacement of the building was significantly reduced if the strength, weight and stiffness of the infilled walls were considered. Further study is needed to evaluate the ductility capacity of the building when considering the strength, weight and stiffness of the infilled walls to more clearly compare the seismic performance among the three cases.

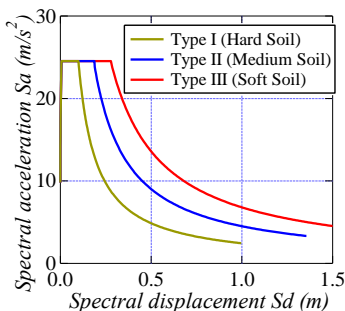


Fig. 20 - Design spectrum in IS 1893

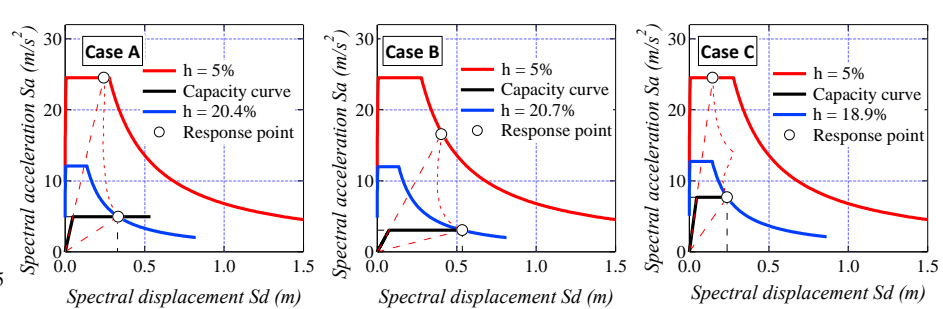


Fig. 21 - Comparison of the response point of each case

## 6. Conclusions

The vibration characteristics of the target building were evaluated via microtremor measurement. Furthermore, experimental studies on brick masonry prism specimens and analytical studies were performed to investigate the effects of the infill walls on the seismic performance of the Nepalese RC building. The major findings of this study are summarized below.

- 1) The natural periods from the analysis considering the strength, weight and stiffness of the brick masonry infill walls had the best agreement with those from the microtremor measurements. This finding shows that the vibration characteristics of Nepalese RC buildings are significantly affected by the presence of brick masonry infill walls.



- 2) The response displacement of the building decreased when the stiffness of the brick masonry infill walls was considered. This finding shows that the brick masonry infill walls significantly affect the inelastic seismic response of the RC buildings.
- 3) Brick masonry infill walls are neglected during the structural design of Nepalese RC buildings. However, it was concluded that the structural performance of RC buildings is significantly affected by the presence of infill walls and should be considered when designing or evaluating the seismic performance of new or existing RC buildings. However, more investigations are necessary, particularly considering the out-of-plane behavior/performance of the infill walls to evaluate their effect on the structural performance of the whole buildings.

## 7. Acknowledgements

The project was funded by J-RAPID (Project title: Field investigation research to improve seismic capacity of new and existing Nepalese buildings, Project leader: Professor Kusunoki Koichi, the University of Tokyo). The authors are greatly thankful for the support.

## 8. References

- [1] United States Geological Survey (USGS) (2015).
- [2] Architectural Institute of Japan (2016). Reconnaissance Report on the 2015 Nepal Gorkha Earthquake.
- [3] Maidiawati, Sanada Y, Konishi D, Tanjung J (2011): Seismic Performance of Nonstructural Brick Walls Used in Indonesian R/C Buildings. *Journal of Asian Architecture and Building Engineering*, **10**(1), 203-210.
- [4] Yamauchi N, Sanada Y, Takahashi E, Nakano Y (2007): Effects of Non-structural Block Infill on Seismic Performance of RC Frame. *Proceedings of the Japan Concrete Institute*, **29**(3),925-930.
- [5] Sungkono, Warnana D.D, Triwulan, Utama W (2011): Evaluation of Buildings Strength from Microtremor Analyses, *International Journal of Civil and Environmental Engineering*, **11**(05),108-114.
- [6] Nepal National Building Code NBC 105,1994.
- [7] Shibata A (2010): *Dynamic analysis of earthquake resistant structures*, Japan.
- [8] Architectural Institute of Japan (2010): Standard for Structural Calculation of Reinforced Concrete Structures, (in Japanese).
- [9] Stafford Smith, B, Carter C (1969): A method of Analysis for Infilled Frames, *Proceedings of the Institution of Civil Engineers*, **44**(1), 31-48.
- [10] Mainstone R J (1971): On the Stiffness and Strengths of Infilled Frames, *Proceedings of Institution of Civil Engineers (ICE). Supplement (iv)*, paper 7360.
- [11] Architectural Institute of Japan (1999): Design Guidelines for Earthquake Resistant Reinforced Concrete Buildings Based on Inelastic Displacement Concept, (in Japanese).
- [12] Kuramoto H, Teshigawara M, Okuzono T, Koshika N, Takayama M, Hori N (2000): Predicting the Earthquake Response of Buildings using Equivalent Single Degree of Freedom System, *Proceedings of 12<sup>th</sup> World Conference on Earthquake Engineering*, Auckland, New Zealand.
- [13] Neupane P, Shrestha S (2015): Comparative Analysis of Seismic Code of Nepal and India for RC Building, *International Journal of Engineering Trends and Technology (IJETT)*, **28**(2),102-105.
- [14] Indian Standard IS 1893 (Part1): 2002.
- [15] Shibata A (2014): *The latest seismic structure analysis*, Japan, 3<sup>rd</sup> edition (in Japanese).